Optimised photocatalytic degradation of a mixture of azo dyes using a $TiO_2/H_2O_2/UV$ process

Soraya Moreno Palácio, Fernando Rodolfo Espinoza-Quiñones, Aparecido Nivaldo Módenes, Diego Ricieri Manenti, Cláudio Celestino Oliveira and Juliana Carla Garcia

ABSTRACT

The aim of the present study was to optimise the photocatalytic degradation of a mixture of six commercial azo dyes, by exposure to UV radiation in an aqueous solution containing TiO_2-P25. Response surface methodology, based on a 3^2 full factorial experimental design with three replicates was employed for process optimisation with respect to two parameters: TiO_2 (0.1–0.9 g/L) and H_2O_2 (1–100 mmol/L). The optimum conditions for photocatalytic degradation were achieved at concentrations of 0.5 g TiO_2/L and 50 mmol H_2O_2/L, respectively. Dye mineralisation was confirmed by monitoring TOC, conductivity, sulfate and nitrate ions, with a sulfate ion yield of 96% under optimal reactor conditions. Complete decolorisation was attained after 240 min irradiation time for all tested azo-dyes, in a process which followed a pseudo-first kinetic order model, with a kinetic rate constant of approximately 0.018 min^{-1}. Based on these results, this photocatalytic process has promise as an alternative for the treatment of textile effluents.

Key words | azo dyes, mineralisation, photocatalytic degradation, sulfate

Soraya Moreno Palácio
Fernando Rodolfo Espinoza-Quiñones
(corresponding author)
Aparecido Nivaldo Módenes
Diego Ricieri Manenti
Postgraduate Program of Chemical Engineering,
Paraná West State University,
rua da Faculdade 645,
Jd. Santa Maria,
85903-000 Toledo, PR,
Brazil
E-mail: f.espinoza@terra.com.br

Cláudio Celestino Oliveira
Juliana Carla Garcia
Postgraduate Program of Chemistry,
Maringá State University,
Av. Colombo 5790,
87020-900, Maringá, PR,
Brazil

INTRODUCTION

Industrial effluents from the textile industry contain a wide variety of colouring agents, such as dyes, inorganic pigments, tannins and lignins; and wastewater pollution from the textile industry has been recognised as a global environmental problem. The most widely used synthetic dyes are azo dyes, which are characterised by the presence of an $-N=N-$ chromophore, as well as other functional groups, such as $-NH_2$, $-OH$, $-COOH$, and $-SO_3H$, which are responsible for fibre fixation and colour enhancement (Molinari et al. 2004).

Over the last decade, several physical and chemical treatment methods have been developed for the degradation or removal of organic pollutants from textile effluents (Palácio et al. 2009; Fiorentin et al. 2010). Among these methods, advanced oxidation processes (AOPs) have been widely utilised for the degradation of refractory organic compounds, including azo dyes in aqueous solution (Tanaka et al. 2000; Gozmen et al. 2003). In particular, heterogeneous photocatalysis, which uses particulate titanium dioxide (TiO_2) suspended in solution, has been applied in order to remove colour from humic acid in water (Bekbolet & Balcioglu 1996) and organic dyes (Zielinska et al. 2003). The colour removal from real textile effluents by means of TiO_2 based photocatalytic method in association with hydrogen peroxide has also been reported by Garcia et al. (2009). In more recent work, the photocatalytic decolorisation and mineralisation of three orange dyes in the presence of TiO_2 nanoparticles were investigated, showing a more efficient use of this process in neutral pH (Khatae et al. 2010).

The mechanism of azo dye wastewater treatment by UV/TiO_2 photocatalysis is as follows: absorption of UV photons ($h\nu > 3.2$ eV; $\lambda < 390$ nm) onto the surface of the TiO_2 semiconductor frees pairs of conduction band electrons (e^-) and valence band holes (h^+) to interact with surrounding molecules, such as adsorbed molecular O_2 (resulting in oxygen ionosorption, and the formation of $O2^{\bullet -}$) and water (resulting in oxidation of OH^- ions and absorption of water molecules in valence band holes). These interactions lead to superoxide protonation, and the formation of hydroperoxyl radicals ($HO_2^{\bullet}$) and H_2O_2 (Gaya & Abdullah 2008). Therefore, effective degradation of organic pollutants is expected to occur close to the catalyst surface,

due to the action of these strong oxidising agents on the dye molecules, which transform them into small inorganic species (Gonçalves *et al.* 2005). In addition, UV/TiO$_2$-based dye degradation systems have been applied, due to their low cost and relatively high chemical stability (Wu 2008).

As a modern effective optimisation tool, the response surface methodology (RSM) that was earlier reported by Myers & Montgomery (2002) could be applied in multi-parametric experiments as found in physical and chemical treatment methods, searching optimal experimental conditions as well as a better understanding of the performance of such treatment systems. In the present work, thus, an optimised TiO$_2$-based photocatalytic degradation of a simulated dyebath solution was investigated by RSM. In addition, the improvement on the efficiency of the dye degradation was evaluated on the basis of the yield of by-products coming from the azo-dye molecule degradation as well as the colour removal and total organic carbon reduction. A kinetic study of colour disappearance was performed in order to provide experimental data for a future reactor modelling.

MATERIALS AND METHODS

Reagents and chemicals

All reagents were of analytical grade and were obtained from Merck. Double distilled water was used to prepare all solutions. The following direct dye standard powders were used to prepare a set of 1.0 g/L pure dyeing stock solutions: Solophenyl orange TGL, Solophenyl blue 71, Solophenyl scarlet BNLE, Solophenyl yellow ARL, Solophenyl black FR and Navy Blue 98. Diluted aqueous solutions containing 50 mg/L pure dye were used to determine the maximum absorbance wavelength of each dye between 190 and 800 nm. To simulate dyebath effluents, a mixture of these aqueous dye solutions was prepared at a concentration of 50 mg/L (each dye).

A TiO$_2$-P25 photocalyst, consisting of 80% anatase and 20% rutile, with a specific BET-surface area of 50 m^2/g, was used for degradation of the simulated dyebath effluent.

Apparatus

Wooden multi-lamp photocatalytic reactor chambers (dimensions of 0.8 m × 0.8 m × 0.5 m) were used for heterogeneous photocatalytic reactions. The reactors contained three high pressure Hg vapour lamps (250 W; similar to street lights); the thick glass covers were removed from the lamps to allow UV irradiation with wavelength above 350 nm. The Hg vapour lamps were positioned 30 cm over a series of three 1.0-L open cylindrical borosilicate vessels. The internal walls of each photocatalytic reactor chamber were covered with highly polished aluminium foil. In addition, each reactor contained two cooling fans and two exhaust vents located on the side walls, which served to maintain the internal reactor temperature at approximately 35 °C.

Analysis and dye characterisation

Photocatalytic degradation was monitored by measuring sample decolorisation as the reduction in dye concentration using a UV–Vis spectrophotometer (Shimadzu 1610). By varying the wavelength from 190 to 800 nm, a molecular absorption spectrum for each type of pure dye solution was measured, exhibiting a broad maximum absorbance wavelength peak at 404, 416, 483, 494.5 and 588 nm for Solophenyl yellow, Solophenyl orange, Solophenyl black, Solophenyl scarlet, and Solophenyl blue, respectively, while the absorbance values for the mixture of dyes at the same wavelengths were measured to be 4.43 (404 nm), 4.45 (416 nm), 3.42 (483 nm), 3.29 (494.5 nm), and 2.99 (588 nm). From the average of absorbance values obtained from triplicate samples, the decolorisation value (ΔAbs) was calculated by the Equation (1).

$$\Delta \text{Abs}(\%) = 100 \frac{[\text{Abs}_0^M - \text{Abs}^M]}{\text{Abs}_0^M} \tag{1}$$

In Equation (1), Abs^M is the average of absorbance values at the maximum absorbance wavelength. Abs_0^M and Abs^M correspond to the values before and after the photocatalytic treatment, respectively.

The pH of the samples was adjusted as required by adding small aliquots of HCl (0.1 mol/L) and NaOH (0.1 mol/L). Mineralisation rates were calculated from the reduction of total organic carbon (TOC), and the oxidation of nitrogen and sulfur organic compounds to nitrate and sulfate ions. All analytical techniques used followed standard methods (APHA, AWWA, WPCF 2005).

Adsorption tests

Adsorption experiments were performed in batch mode. 200 mL mixture solutions containing 50 mg/L standard

dye solution and 200 mg of TiO_2 were used to evaluate the performance of the adsorption process between pH 3 and 11. All sample mixtures were homogenised in an ultrasonic bath for 60 min in the dark, which improved the adsorption process and enabled attainment of adsorption equilibrium. At 10-min time intervals, sample aliquots (5 mL) were withdrawn. The solid phase was separated from the liquid phase using a 0.22 µm polyethylene filtration system. The dye concentration in the filtered sample was then determined spectrophotometrically at the maximum absorbance wavelength for each standard dye.

Factorial design

Based on the best adsorption conditions, the influence of H_2O_2 and TiO_2 was investigated at pH 3 using RSM (Myers & Montgomery 2002), in order to improve the reaction efficiency and sulfate yield. For this purpose, a full 3^2 factorial experimental design was applied to analyse the photocatalytic experiments, which were performed for 360 min. The experimental design combined two-levels and one point at the centre of each experimental region, which was previously chosen from preliminary tests: TiO_2 (0.1, 0.5 and 0.9 g/L) and H_2O_2 (0.001, 0.01 and 0.1 mol/L). In spite of being a good indicator for monitoring the progress of dye mineralisation, the nitrate concentration is not a suitable response variable for optimised photocatalytic degradation, due to the total amount of nitrogen in azo-dye molecules being converted into different nitrogen forms such as nitrate, nitrite, ammonia and N_2 gas as commented in the mineralisation analysis below. A second-order model (see Equation (2), where q_1 and q_2 represent the concentration of TiO_2 and H_2O_2, respectively) was used to model the photocatalytic data, by considering sulfate yield as a response variable. The model was validated by analysis of variance (ANOVA), enabling assessment of the interaction between the concentration of TiO_2 and H_2O_2.

$$R = a_0 + \sum_{i=1}^{2} a_i q_i + \sum_{i=1}^{2} \sum_{j=1}^{2} b_{ij} q_i q_j + \sum_{i=1}^{2} \sum_{j=1}^{2} \sum_{k=1}^{2} c_{ijk} q_i q_j q_k$$
$$+ \sum_{i=1}^{2} \sum_{j=1}^{2} w_{ij} q_i^2 q_j^2 \qquad (2)$$

In Equation (2), R – is the experimental response, q – is a set of reactor operating parameter values, a_0 – is a constant, a – is a set of coefficients for the linear terms; and b, c and

w – are weight coefficients representing the various types of interactions between the reactor operating parameter values.

Photocatalytic experiments

A simulated dyebath solution was made containing the following dyes: Solophenyl orange TGL, Solophenyl blue 71, Solophenyl scarlet BNLE, Solophenyl yellow ARL, Solophenyl black FR and Navy Blue 98. The dyebath solution was mixed with a TiO_2 photocatalyst suspension in a 0.5 L reaction mixture, and the pH was adjusted to 3.0 (the pH at which the highest dye adsorption was observed). In all cases, reaction mixtures were previously homogenised in an ultrasonic bath for 15 min in the dark, taking into consideration results from preliminary adsorption tests. In the photo reactor chamber, each sample was magnetically stirred at 300 rpm and exposed to UV light. A 5 mL aliquot was collected from each reactor at 60 min intervals; for each aliquot, catalyst was separated from the solution using a 0.22 µm polyethylene filter. Dye concentration was then determined spectrophotometrically at the maximum absorbance wavelength for each standard dye.

Reaction kinetics were studied for reactions conducted at the optimal H_2O_2 and TiO_2 concentrations predicted by the factorial design: dye concentrations and UV intensity were held constant, and radiation time was varied from 60 to 360 min. In addition, intermediate products were also estimated from TOC values, and by monitoring the oxidation of nitrogen and sulfur organic compounds to nitrate and sulfate ions. All experiments were performed in triplicate.

RESULTS AND DISCUSSION

Adsorption tests

It was observed that the maximum dye adsorption efficiency (80%) was achieved in the first 10 min when a solution pH of 3 was used. In addition, the amounts of dye adsorbed by the TiO_2 decreased when the solution pH was increased, in agreement with the previous results reported by Zielinska *et al.* (2003).

Statistical analysis

Based on results from 3^2 full factorial experiments, an optimisation procedure was performed using sulfate ion yield as a response variable. Results from this optimisation

procedure are summarised in Table 1. As can be seen, minimum and maximum values were approximately 9 and 84 mg/L, respectively.

A predicted second order model for sulfate ion yield (see Equation (3)) was obtained using the software STATISTICA 7.0. This model fit the planned experimental data adequately, with a good correlation coefficient for predicted sulfate ion concentrations. The statistical significance of the linear and quadratic effects of q_1 (TiO₂) and q_2 (H₂O₂), and their combined action on the yield of sulfate ions, was confirmed by application of a two-way ANOVA test on the predicted model (95% confidence level; $p <$ 0.05) (see Table 2).

$$[SO_4^{2-}] = 56 + 11q_1 + 29q_2 - 3.3q_1q_2 + 0.7q_1^2 + 7q_2^2 \\ + 1.8q_1q_2^2 - 1.1q_1^2q_2 + 2.3q_1^2q_2^2 \tag{3}$$

Based on modelling results for sulfate ion yield, the linear coefficients associated with TiO₂ (q_1) and H₂O₂ (q_2) assume positive values, suggesting that increasing both reactor parameters could improve sulfate ion yield. However, the negative and positive coefficients obtained for the combined actions of TiO₂ and H₂O₂ indicate opposing effects on sulfate ion yield, suggesting that intermediate values for both

reactor parameters would be optimal. Based on the planned experimental data, a response function for sulfate ion yield was built in a 3D graph (see Figure 1), which was used to visualise the maximal sulfate ion yield. Maximal sulfate yield (approximately 130 mg/L) was achieved when the photoreactor was operated using the following conditions: 0.5 g/L TiO₂ and 0.05 mol/L H₂O₂.

Mineralisation analysis

Decolorisation of the simulated dyebath solution was measured by monitoring the absorbance reduction factor at the maximum absorbance wavelength of each dye. Almost 100% colour removal was attained for UV irradiation times >240 min (Figure 2(a)), when photocatalytic degradation experiments were performed at optimal reactor conditions (0.5 g TiO₂/L and 0.05 mol H₂O₂/L).

The total yield of each expected byproduct was stoichiometrically calculated, taking into consideration the initial amount of each dye (50 mg/L) in the simulated dye bath samples, the mineralisation equation of each type of dye molecule, and mass balance analysis (Malato *et al.* 2003) (see Equations (4)–(9)). Theoretical sulfate ion yields were 16.5, 16.3, 18.6, 13.2, 21.6, and 15.6 mg/L from Solophenyl orange TGL ($C_{25}H_{33}ClN_6O_6S_2$), Solophenyl scarlet BNLE ($C_{44}H_{32}N_{10}Na_4O_{16}S_4$), Solophenyl blue 71 ($C_{40}H_{23}N_7Na_4O_{13}S_4$), Solophenyl black FR ($C_{44}H_{32}N_{13}Na_3O_{11}S_3$), Solophenyl yellow ARL ($C_{48}H_{26}N_8Na_6O_{18}S_6$), and Navy Blue 98 ($C_{38}H_{24}N_5Na_3O_{13}S_3$), respectively, resulting in a total sulfate ion concentration of 101.8 mg/L; whereas the total nitrate ion concentration is expected to be 151.4 mg/L.
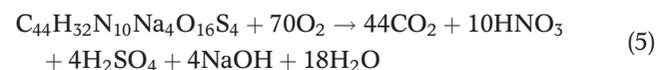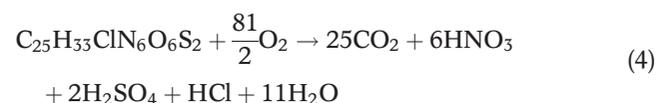
Table 1 | A 3² full factorial design with three replicates

Run	Reactor parameters		Yield of [SO_4^{2-}] (mg/L)		
	q_1 (g/L)	q_2 (mol/L)	Y_1	Y_2	Y_3
1	0.10	0.001	9.23	9.13	9.34
2	0.10	0.01	21.56	20.87	21.98
3	0.10	0.1	74.36	74.13	74.59
4	0.50	0.001	36.47	37.32	35.45
5	0.50	0.01	63.91	62.77	64.11
6	0.50	0.1	84.12	83.81	84.10
7	0.90	0.001	65.93	65.27	67.90
8	0.90	0.01	66.16	64.84	67.48
9	0.90	0.1	68.58	69.95	67.90

$$C_{25}H_{33}ClN_6O_6S_2 + \frac{81}{2}O_2 \rightarrow 25CO_2 + 6HNO_3 \\ + 2H_2SO_4 + HCl + 11H_2O \tag{4}$$

$$C_{44}H_{32}N_{10}Na_4O_{16}S_4 + 70O_2 \rightarrow 44CO_2 + 10HNO_3 \\ + 4H_2SO_4 + 4NaOH + 18H_2O \tag{5}$$

Table 2 | Two-way ANOVA test of the predicted model for SO_4^{2-} yield

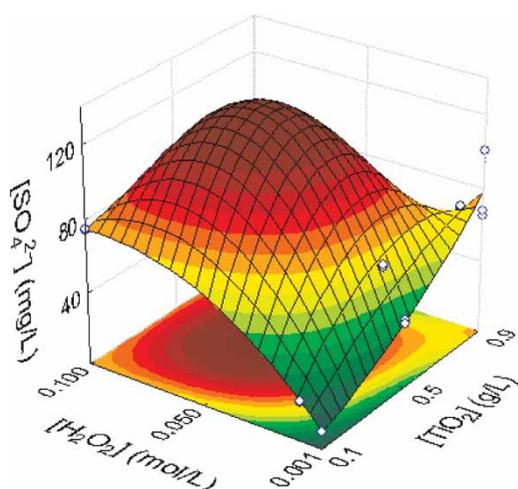|	Sum of square errors	Degrees of freedom	Mean square error	F		Significance level
				Calculated	Statistical	
Regression	17,087.58	8	2,135.95	47.92	2.51	<0.01
Residues	802.33	18	44.57			
Total	17,889.91	26				

Figure 1 | Experimental response surface results for SO_4^{2-} yield from the photocatalytic degradation of a simulated dyebath solution.
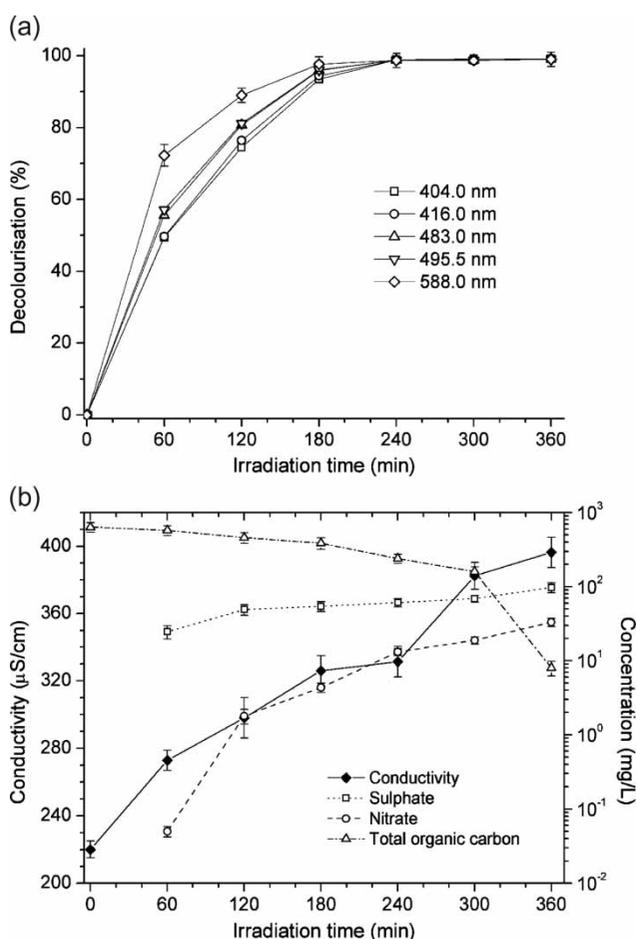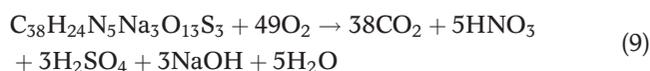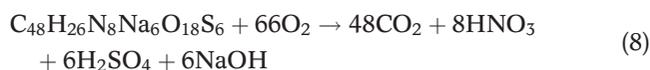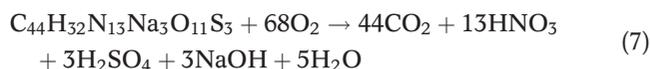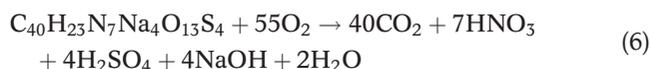

Figure 2 | (a) Percent colour removal at the maximum absorbance wavelength of each dye and (b) changes in the mineralisation of the simulated dyebath solution as a function of monitored parameters vs. irradiation time. Reactions were performed under optimal reactor conditions.

$$C_{40}H_{23}N_7Na_4O_{13}S_4 + 55O_2 \rightarrow 40CO_2 + 7HNO_3 + 4H_2SO_4 + 4NaOH + 2H_2O \tag{6}$$

$$C_{44}H_{32}N_{13}Na_3O_{11}S_3 + 68O_2 \rightarrow 44CO_2 + 13HNO_3 + 3H_2SO_4 + 3NaOH + 5H_2O \tag{7}$$

$$C_{48}H_{26}N_8Na_6O_{18}S_6 + 66O_2 \rightarrow 48CO_2 + 8HNO_3 + 6H_2SO_4 + 6NaOH \tag{8}$$

$$C_{38}H_{24}N_5Na_3O_{13}S_3 + 49O_2 \rightarrow 38CO_2 + 5HNO_3 + 3H_2SO_4 + 3NaOH + 5H_2O \tag{9}$$

Based on the formation of intermediate products, the $-N=N-$ bond in the dye molecules may be easily cleavable by photocatalytic processes, resulting in the formation of acids with or without hydroxyl groups, and sulfate and nitrate ions. Solophenyl scarlet BNLE, Solophenyl blue 71, Solophenyl black FR, Solophenyl yellow ARL, and Navy Blue 98 are expected to follow a similar degradation pathway, also yielding sulfate and nitrate ions. In contrast, Solophenyl orange TGL may degrade via a different pathway, yielding chlorine as the final product.

The total nitrate concentration (151.4 mg/L) was not confirmed experimentally, probably because of partial transformation of the nitrate ions to other nitrogen forms. For example, generated nitrate ions could be attacked by hydroxyl radicals, resulting in the formation of ammonia. In addition, part of the total nitrogen content might be lost as N_2, since the azo-dye group ($-N=N-$) could act as an N_2 precursor, and some nitrogen atoms within the azo-dye groups are in neutral form as N_2 (Karkmaz *et al.* 2004). The formation of N_2 from the $-N=N-$ azo-dye group can be represented by Equations (10) and (11):

$$R-N=N-R' + OH^{\bullet} \rightarrow R-N=N^{\bullet} + R'-OH \tag{10}$$

$$R-N=N^{\bullet} \rightarrow R^{\bullet} + N_2 \tag{11}$$

The progress of dye mineralisation was monitored by measuring TOC, conductivity, and the concentration of sulfate and nitrate ions, as shown in Figure 2(b). The behaviour of these response parameters was analysed by varying the UV irradiation time from 60 to 360 min under optimal experimental conditions. Interestingly, the amount of mineralised dye molecules was observed to increase with increasing irradiation time. In addition, increased conductivity was also observed, suggesting an increase in

the amount of anions and cations in the medium. This result was confirmed by the increased sulfate and nitrate ion concentrations observed following photocatalytic degradation of the dyes. Another indicator of dye mineralisation is the observed reduction in the amount of total organic carbon. Furthermore, a high amount of nitrogen could be present in the form of other compounds, such as ammonia, since a 22% reduction in nitrate ion concentration is expected versus the theoretical value (151.4 mg/L). Nitrite ions are also expected to form from ammonia ions, albeit at a low rate (Hidaka *et al.* 1995). Moreover, because the TiO$_2$ surface is positively charged in acidic media, the amount of anions (e.g. NO$_3^-$ and SO$_4^{2-}$) adsorbed on the TiO$_2$ surface should also be taken into account (Karkmaz *et al.* 2004).

Kinetic study

In the present study, kinetic degradation data for decolorisation was modelled by zero-, pseudo first- and second-order kinetic models, as shown in Equation (12), in order to predict the degradation behaviour of a mixture of dyes under optimal experimental conditions (0.5 g TiO$_2$/L and 0.05 mol H$_2$O$_2$/L).

$$\frac{\mathrm{d}C}{\mathrm{d}t} = k_{\mathrm{OH}}[\mathrm{OH}^\bullet]C^\alpha = k_{a\mathrm{p}}C^\alpha \tag{12}$$

where C is the absorbance of the sample, k_{OH} is the reaction rate constant, $k_{a\mathrm{p}}$ is the kinetic constant and α is the reaction order.

Based on the correlation coefficient at five maximum absorption characteristic wavelength bands of the dyes, a pseudo first-order kinetic model was found to fit the kinetic data better than the other models. From linear fits of the experimental data, the kinetic rate constant was determined to be approximately 0.018 min^{-1} for all investigated wavelengths, suggesting that photocatalytic dye degradation is a slow process, which requires approximately 38.5 min for a 50% reduction in colour, and 240 min for complete decolorisation of dye mixture samples.

CONCLUSION

In an effort to relate results from our present study to real-life textile effluents, we investigated the photocatalytic degradation of a simulated dyebath solution and monitored dye molecule mineralisation. Response surface methodology, a powerful statistical tool, was used to determine the optimal photocatalytic reactor conditions. Based on a 3^2 full factorial experimental design and 3-D surface analysis of sulfate ion concentration, maximal yield is expected when the reactor is operated at 0.5 g TiO$_2$/L and 0.05 mol H$_2$O$_2$/L. Thus, 130 mg/L sulfate ion is expected after azo dye mineralisation. Furthermore, based on mineralisation equations of the tested dye molecules, the $-\mathrm{N}=\mathrm{N}-$ bond within the tested azo-dye molecules might be cleaved during the photocatalytic process, resulting in the formation of sulfate (101.8 mg/L) and nitrate ions (151.4 mg/L). By monitoring TOC, conductivity and the yield of sulfate and nitrate ions, all azo-dyes were found to be efficiently degraded to simpler compounds. Complete decolorisation was observed after 240 min irradiation time and a pseudo-first kinetic order model was found to fit the decolorisation data well. Based on these results, further investigations are in progress to analyse the potential commercial use of photocatalytic degradation of real textile effluents as an alternative means of dyehouse effluent treatment.

REFERENCES

APHA, AWWA, WPCF 2005 *Standard Methods for the Examination of Water and Wastewater*, 21st edition. American Public Health Association, Washington, DC.

Bekbolet, M. & Balcioglu, I. 1996 Photocatalytic degradation kinetics of humic acid in aqueous TiO$_2$ dispersions: the influence of hydrogen peroxide and bicarbonate ion. *Water Science and Technology* **34** (9), 73–80.

Fiorentin, L. D., Trigueros, D. E. G., Módenes, A. N., Espinoza-Quiñones, F. R., Pereira, N. C., Barros, S. T. D. & Santos, O. A. A. 2010 Biosorption of reactive blue 5G dye onto drying orange bagasse in batch system: kinetic and equilibrium modeling. *Chemical Engineering Journal* **163**, 68–77.

Garcia, J. C., Simionato, J. I., Silva, A. E. C., Nozaki, J. & Souza, N. E. 2009 Solar photocatalytic degradation of real textile effluents by associated titanium dioxide and hydrogen peroxide. *Solar Energy* **83**, 316–322.

Gaya, U. I. & Abdullah, A. H. 2008 Heterogeneous photocatalytic degradation of organic contaminants over titanium dioxide: a review of fundamentals, progress and problems. *Journal of Photochemistry and Photobiology C: Photochemistry Reviews* **9**, 1–12.

Gonçalves, M. S. T., Pinto, E. M. S., Nkeonye, P. & Oliveira-Campos, A. M. F. 2005 Degradation of C.I. reactive orange 4 and its simulated dyebath wastewater by heterogeneous photocatalysis. *Dyes and Pigments* **64**, 135–139.

Gozmen, B., Oturan, M. A., Oturan, N. & Erbatur, O. 2003 Indirect electrochemical treatment of bisphenol A in water via electrochemically generated Fenton's reagent. *Environmental Science and Technology* **37**, 3716–3723.

Hidaka, H., Nohara, K., Zhao, J., Pelizzetti, E. & Serpone, N. 1995 Photodegradation of surfactants XIV. Formation of NH$_4^+$ ano NO$_3^-$ ions for the photocatalysed mineralization of nitrogen-containing cationic, non-ionic and amphoteric surfactants. *Journal of Photochemistry and Photobiology A: Chemistry* **91**, 145–152.

Karkmaz, M., Puzenat, E., Guillard, C. & Herrmann, J. M. 2004 Photocatalytic degradation of the alimentary azo dye amaranth. Mineralization of the azo group to nitrogen. *Applied Catalysis B: Environmental* **51**, 183–194.

Khataee, A. R., Pons, M. N. & Zahraa, O. 2010 Photocatalytic decolorisation and mineralisation of orange dyes on immobilised titanium dioxide nanoparticles. *Water Science and Technology* **62** (5), 1112–1120.

Malato, S., Blanco, J., Campos, A., Cáceres, J., Guillard, C., Herrmann, J. M. & Fernández-Alba, A. R. 2003 Effect of operating parameters on the testing of new industrial titania catalysts at solar pilot plant scale. *Applied Catalysis B: Environmental* **42**, 349–357.

Molinari, R., Pirillo, F., Falco, M., Loddo, V. & Palmisano, L. 2004 Photocatalytic degradation of dyes by using a membrane reactor. *Chemical Engineering and Processing* **43**, 1103–14.

Myers, R. H. & Montgomery, D. C. 2002 *Response Surface Methodology: Process and Product Optimization using Designed Experiments*, 2nd edition. John Wiley & Sons, New York.

Palácio, S. M., Espinoza-Quiñones, F. R., Módenes, A. N., Oliveira, C. C., Borba, F. H. & Silva Jr., F. G. 2009 Toxicity assessment from electro-coagulation treated-textile dye wastewaters by bioassays. *Journal of Hazardous Materials* **172**, 330–337.

Tanaka, K., Padermpole, K. & Hisanaga, T. 2000 Photocatalytic degradation of commercial azo dyes. *Water Research* **34**, 327–333.

Wu, C. H. 2008 Effects of operational parameters on the decolorization of C.I. Reactive Red 198 in UV/TiO$_2$-based systems. *Dyes and Pigments* **77**, 31–38.

Zielinska, B., Grzechulaka, J., Morawski, A. W. & Kalenczuk, R. J. 2003 The pH influence on photocatalytic decomposition of organic dyes over A11 and P25 titanium dioxide. *Applied Catalysis B: Environmental* **45**, 293–300.